DOI: 10.1002/chem.201003726

Synthesis and Characterization of a Symmetric Bis(7-hydroxyflavylium) Containing a Methyl Viologen Bridge

Ana M. Diniz, Carlos Pinheiro, Vesselin Petrov, A. Jorge Parola, and Fernando Pina*[a]

Abstract: A symmetric bis(flavylium) constituted by two 7-hydroxyflavylium moieties linked by a methylviologen bridge was synthesized. The thermodynamic and kinetics of the network of chemical reactions involving bis(flavylium) and the model compound 7-hydroxy-4′-methylflavylium was completely characterized by means of direct and reverse pH jumps (stopped flow) and flash photolysis. Both compounds follow the usual pH-dependent network of chemical reactions of flavylium derivatives. The equilibrium species of the model compound are the flavylium cation (acidic species) and the *trans*-chalcone (basic species) with an apparent $pK'_a = 2.85$. In the case of the bis(flavylium) it was possible to characterize by ^1H NMR spectroscopy three species with different degrees of isomerization: all flavylium, flavylium-*trans*-chalcone, and all *trans*-chalcone. Representation of the time-dependent mole fraction distribution of these three forms after a pH jump from equilibrated solutions of all-flavylium cation (lower pH values) to higher pH values, shows that formation of *trans*-chalcone is not completely stochastic (two independent isomerizations), the isomerization of one flavylium showing a small influence on the isomerization of the other. The radical of the methyl viologen bridge is formed upon reduction of the bis(*trans*-chalcone) with dithionite. The system is reversible after addition of an oxidant in spite of the occurrence of some decomposition.

Keywords: electrochemistry · flavylium · multistates · photochromism · viologen

Introduction

Synthetic flavylium salts constitute a versatile family of compounds possessing the same basic structure of anthocyanins, the ubiquitous compounds responsible for most of the red and blue colors of flowers and fruits.[1–5] Their physical–chemical properties are greatly dependent on the nature and position of the functional groups attached to the 2-phenyl-1-benzopyrylium skeleton.[5] However, independent on their structure and provenience, natural or synthetic, flavylium derivatives follow in general the same network of chemical reactions previously established by Dubois, Brouillard, and McClelland, exemplified in Scheme 1 for 7-hydroxyflavylium.[6]

In acidic media, the flavylium cation, $\mathbf{AH^+}$, is the thermodynamically stable species. When the pH is raised, other species are formed: the quinoidal base **A**, which is generally a transient species formed immediately upon deprotonation of the phenol group, the hemiketal **B2**, through hydration in the 2-position of the flavylium cation. Tautomerization of **B2** leads to the formation of the *cis*-chalcone **Cc**, through a ring-opening process, and finally, the *cis*/*trans* isomerization results in the formation of the *trans*-chalcone **Ct**. The following set of equations [Eq. (1—4)] accounts for the sequence of reactions shown in Scheme 1.

$$\mathbf{AH^+} + H_2O \rightleftharpoons \mathbf{A} + H_3O^+ \qquad K_a \text{ Proton transfer} \tag{1}$$

$$\mathbf{AH^+} + 2\,H_2O \rightleftharpoons \mathbf{B2} + H_3O^+ \qquad K_h \text{ Hydration} \tag{2}$$

$$\mathbf{B2} \rightleftharpoons \mathbf{Cc} \qquad K_t \text{ Tautomerization} \tag{3}$$

$$\mathbf{Cc} \rightleftharpoons \mathbf{Ct} \qquad K_i \text{ Isomerization} \tag{4}$$

Equations (1) to (4) can be substituted by a single acid–base equilibrium.

$$\mathbf{AH^+} + H_2O \rightleftharpoons \mathbf{CB} + H_3O^+ \qquad K'_a = \frac{[\mathbf{CB}][H_3O^+]}{[\mathbf{AH^+}]} \tag{5}$$

$$\begin{aligned} K'_a &= K_a + K_h + K_hK_t + K_hK_tK_i \\ [\mathbf{CB}] &= [\mathbf{A}] + [\mathbf{B2}] + [\mathbf{Cc}] + [\mathbf{Ct}] \end{aligned} \tag{6}$$

It is important to stress that in acidic and neutral media the conversion of flavylium into the chalcones takes place through the hydration reaction [Eq. (2)]. The neutral quinoidal base **A** does not hydrate under these conditions (although it can form the hemiketal in basic media by hydroxylation) and thus it is a kinetic product that evolves towards

[a] A. M. Diniz, Dr. C. Pinheiro, Dr. V. Petrov, Dr. A. J. Parola, Prof. F. Pina
REQUIMTE
Departamento de Química
Faculdade de Ciências e Tecnologia
Universidade Nova de Lisboa
2829-516 Caparica (Portugal)
Fax: (+35) 1212948550
E-mail: fjp@dq.fct.unl.pt

Supporting information for this article is available on the WWW under http://dx.doi.org/10.1002/chem.201003726.

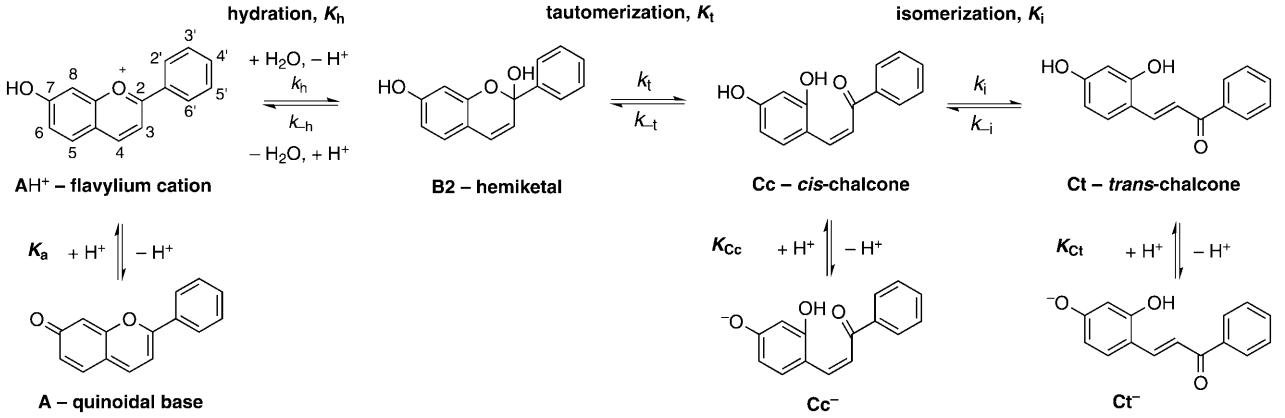

Scheme 1. Chemical reaction network of flavylium salts exemplified for 7-hydroxyflavylium.

chalcones only through the hydration of the flavylium cation.

In contrast with anthocyanins, in which **CB** is mainly constituted by the species **B2**,[7] in many synthetic flavylium compounds **Ct** is the major species at moderately acidic to neutral solutions, which has led to the exploitation of these compounds as photochromic systems.[5,8] In the case of 7-hydroxyflavylium, as in most flavylium compounds, irradiation of **Ct** leads to the primary photochemical product **Cc**.[6] The primary photoproduct tends to revert back to **Ct** (in the absence of a *cis*/*trans* isomerization barrier) or to give the colored species $\mathbf{AH^+}$ or **A**, depending on pH. The efficiency of the photochromic system (considering formation of colored species) is thus dependent on the competition between a forward reaction to give $\mathbf{AH^+}$ or **A** and a backward reaction to recover **Ct**. The colored species resulting from the irradiation revert back to the equilibrium defining a photochromic system. However, some flavylium compounds exhibit high *cis*/*trans* isomerization barriers facilitating the efficiency of the appearance of $\mathbf{AH^+}$/**A** and leading to high lifetimes of the photochemical products by preventing or retarding the thermal back reaction. In this last case, the system can be viewed as a model for optical memories capable of read–write–erase.[9–13]

Besides their role as biological dyes, the flavylium chromophores have acquired importance in materials science applications. In this framework, it would be interesting to extend the network of reactions to include a redox responsive moiety. The viologen was selected due to its well-characterized reversible redox behavior that would allow the enlargement of the possible number of available states and to respond to electric stimuli. In this work, a bis(flavylium) compound possessing two 7-hydroxyflavylium units linked by a methyl viologen bridge in the 4′-position was synthesized to study the mutual effect of two covalently linked photochromic systems and to characterize the redox behavior of the viologen bridge.

Results and Discussion

Synthesis: The synthesis of flavylium compounds is usually achieved through the acid-catalyzed condensation of acetophenones with benzaldehydes, by following a method early introduced by Robinson[14] and slightly modified by Katritzky et al.[15] The synthetic pathway to obtain de desired bis(flavylium) **3** is described in Scheme 2. Bromination of 4′-methylacetophenone yielded 4′-bromomethylacetophenone that was reacted with 4,4′-bipyridine to give bis(acetophenone) **2** in 83% yield. The synthesis of **2** was adapted from a procedure previously described by Porter et al.[16] to prepare extended viologens. Initially, only the symmetric compound was synthesized but by monoalkylation of 4,4′-bypiridine, unsymmetrical moieties could be obtained (not studied in this work). Compound **2** was condensed with 2,4-dihydroxybenzaldehyde under strongly acidic conditions[14,15] to give the desired viologen-bridged bis(flavylium) **3** with a global yield of 48%.

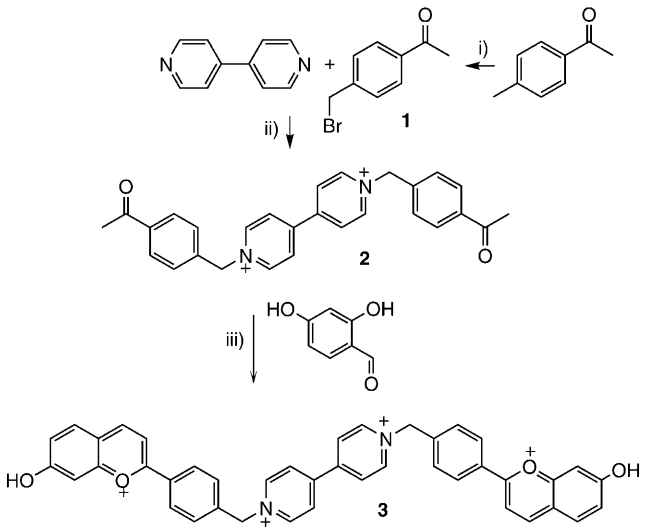

Scheme 2. Synthesis of bis(flavylium) **3** containing a viologen bridge: i) NBS/AIBN/CCl_4, 83%; ii) DMF/reflux, 96%; iii) CH_3COOH/H_2SO_4, 60%. NBS = *N*-bromosuccinimide; AIBN = azobisisobutyronitrile.

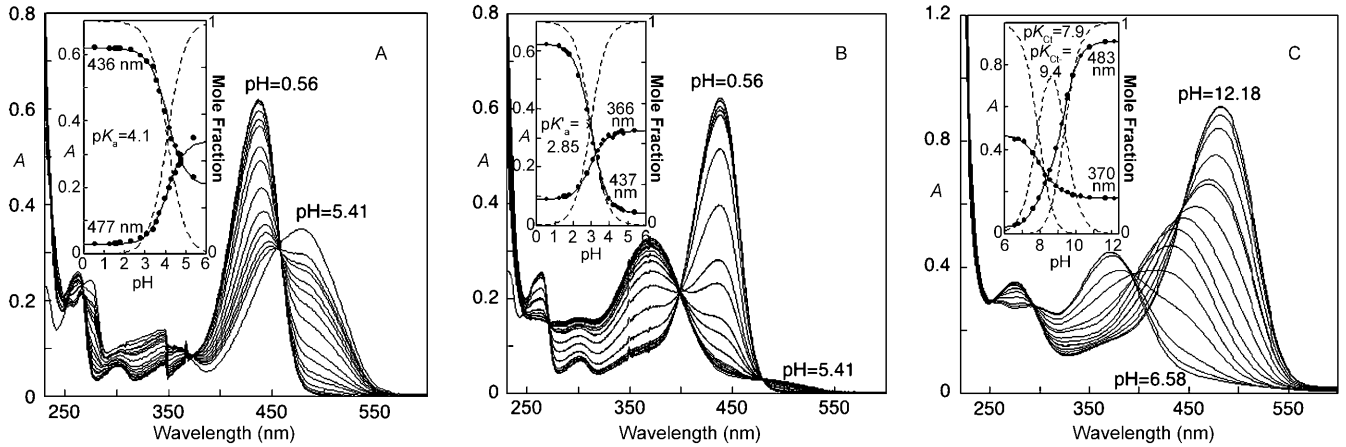

Figure 1. UV/Vis spectral variations occurring upon a pH jump from a stock solution of the model compound **4** at pH 1 (6.4×10^{-5} M) to higher pH values: Spectra recorded immediately after the pH jump (<1 min after adding base) (A) and upon thermodynamic equilibrium being reached (~24 h) (B). Spectral variations upon reverse pH jumps of a solution at pH 12 ($\mathbf{Ct}^{2-}$) to less basic pH values leading to the protonation of the *trans*-chalcones are shown in (C). Insets: fittings (——) of the absorbance values (●) at the specified wavelengths superposed to the mole fraction distribution of species (-----).

For comparative studies, the model compound 7-hydroxy-4′-methylflavylium tetrafluoroborate (**4**) salt was prepared by condensation of 2,4-dihydroxybenzaldehyde with 4′-methylacetophenone in the presence of acetic anhydride and tetrafluoroboric acid with a yield of 27%.

Model compound: 7-hydroxy-4′-methylflavylium tetrafluoroborate (4): The network of chemical reactions of model compound **4** was characterized by following an experimental strategy that consists of the study of the pH-dependent thermodynamic equilibria and the kinetics that result from a perturbation of the system by pH jumps and by light.

The changes in absorption spectra upon direct pH jumps from stock solutions of model compound **4** at pH 1.0 ($\mathbf{AH}^+$) to higher pH values are shown in Figure 1A and B.

In Figure 1A the absorption spectra were taken circa 30 seconds after the pH jump. The shape and position of the bands clearly indicate the formation of the quinoidal base allowing us to calculate $pK_a=4.1$ [Eq. (1)]. Figure 1B shows the pH-dependent absorption of the equilibrated solutions after one day in the dark, leading to $pK'_a=2.85$. These values compare with $pK_a=3.55$ and $pK'_a=2.70$ for 7-hydroxyflavylium.[6] The slightly lower acidity and higher pK'_a of **4** relatively to 7-hydroxyflavylium are consequences of the electron-donor properties of the methyl substituent at the 4′-position relative to the proton.

On the other hand, pH jumps to high pH values (pH>12) lead to the formation of the ionized *trans*-chalcone $\mathbf{Ct}^{2-}$, as observed for similar flavylium compounds.[17] This species can be titrated back to acidic pH, forming $\mathbf{Ct}^-$ and **Ct** with pK_a values of 9.4 and 7.9, as shown in Figure 1C. If the titration continues to more acidic pH values (not shown) formation of flavylium takes place because it is the stable species in acidic medium, as seen in Figure 1B.

The kinetics of the formation of the equilibrium species from direct pH jumps is pH-dependent corresponding to the disappearance of the flavylium cation to form **Ct**, see for example, the spectral variations that follow a pH jump from an equilibrated solution at pH 1 to 3.2 (Figure 2A).

Representation of the rates of the direct pH jumps as a function of pH leads to the previously described[18] bell-shaped curve characteristic of the compounds lacking a high thermal *cis*/*trans* isomerization barrier (Figure 2B). These kinetics can be accounted for by Equation (7).[18]

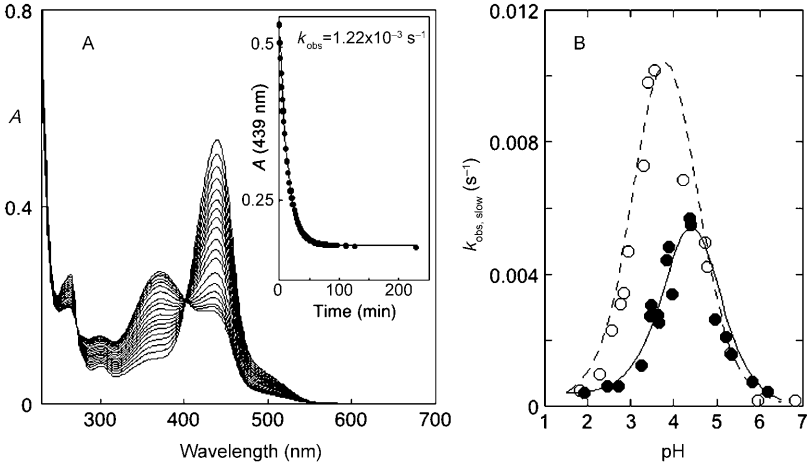

Figure 2. Time evolution of UV/Vis spectra upon a pH jump from a stock solution of compound **4** at pH 1 (6.4×10^{-5} M) to pH 3.2 (A); inset: fitting of the absorbance at 439 nm with a single exponential allows us to calculate k_{obs} at pH 3.2. Similar measurements at several pH values leads to k_{obs} rate constants that plotted against pH lead to bell-shaped curves for both model compound **4** (●) and bis(flavylium) **3** (○).

$$k_{obs} = \frac{\frac{[H^+]}{[H^+]+K_a} K_h K_t k_i + k_{-i}[H^+]}{\frac{k_i K_t}{k_{-h}} + [H^+]} \quad (7)$$

Fitting of the data in Figure 2 (see ●) with Equation (7) was achieved for $K_h K_t k_i = 8.1 \times 10^{-7}$ M s^{-1}, $k_{-i} = 5.0 \times 10^{-4}$ s^{-1}, and $k_i K_t / k_{-h} = 3.7 \times 10^{-5}$ M.

Photochemistry

Continuous irradiation: Continuous irradiation of aqueous solutions of **Ct** at different pH values with 365 nm light causes spectral changes as shown in Figure 3A (pH 4.3) and B (pH 5.39). In both cases, the disappearance of the **Ct** to give a mixture of $\mathbf{AH^+}$ and **A** in Figure 3A and practically only **A** in Figure 3B is clear. This is easily explained by means of Equation (1) and the data reported in Figure 1A, ($pK_a = 4.1$).

The quantum yield is pH-dependent and can be approximately given by Equation (8).[18]

$$\Phi = \Phi_{int} \frac{\frac{k_{-h}[H^+]}{1+K_t}}{\frac{k_{-h}[H^+]}{1+K_t} + \frac{k_i K_t}{1+K_t}} = \Phi_{int} \frac{[H^+]}{[H^+] + \frac{k_i K_t}{k_{-h}}} \quad (8)$$

In Equation (8) it is assumed that hemiketal **B2** and *cis*-chalcone **Cc** are in fast equilibrium. Formation of the colored species ($\mathbf{AH^+}$ or **A**) upon irradiation of **Ct** to give **Cc** is the product of the intrinsic quantum yield of the photoisomerization reaction, Φ_{int}, by the efficiency of formation of $\mathbf{AH^+}$ from **Cc** (ratio between the rate at which $\mathbf{AH^+}$ or **A** is formed from **Cc** and the rates of all processes contributing for the disappearance of **Cc**). Fitting was achieved for $\Phi_{int} = 0.45$ and $k_i K_t / k_{-h} = 4.1 \times 10^{-5}$ M, this last value is in good agreement with the fitting obtained with Equation (7).

Pulsed irradiation: Pulsed radiation is a powerful complementary technique to study the flavylium reaction network since it does not need any pH modification and is a source of kinetic information as shown in Figure 4, in which equilibrated solutions containing **Ct** were irradiated. After the flash, the system can be monitored at a wavelength at which **Ct** absorbs (Figure 4A) and at the flavylium or quinoidal base absorptions depending on pH (Figure 4B). In Figure 4A, a bleaching is observed immediately after the flash that corresponds to the disappearance of **Ct** to give **Cc**, which is known to possess a lower absorption coefficient compared to **Ct**. The second process corresponds to the recovery of some **Ct** absorption as a result of the thermal back reaction from **Cc** to **Ct** in competition with flavylium/quinoidal base formation observed in Figure 4B. These two processes are parallel reactions and the observed rate constant, k_{obs}, is the sum of both. In other words, the rate constant measured at 365 (**Ct**) and 436 nm ($\mathbf{AH^+}$/**A**) is the same, within experimental error, as expected. The $[H^+]$ dependence of this process is represented in Figure 4C. At high proton concentrations, the hydration/dehydration reaction [Eq. (2)] is faster than the tautomerization [Eq. (3)] due to its direct dependence on $[H^+]$ and the rate-determining step of the process is the tautomerization. As soon as **B2** is formed from **Cc** it immediately dehydrates to give $\mathbf{AH^+}$, and the rate is controlled by the value of k_{-t} [Eq. (9)]. At lower proton concentrations, the rate-determining step is

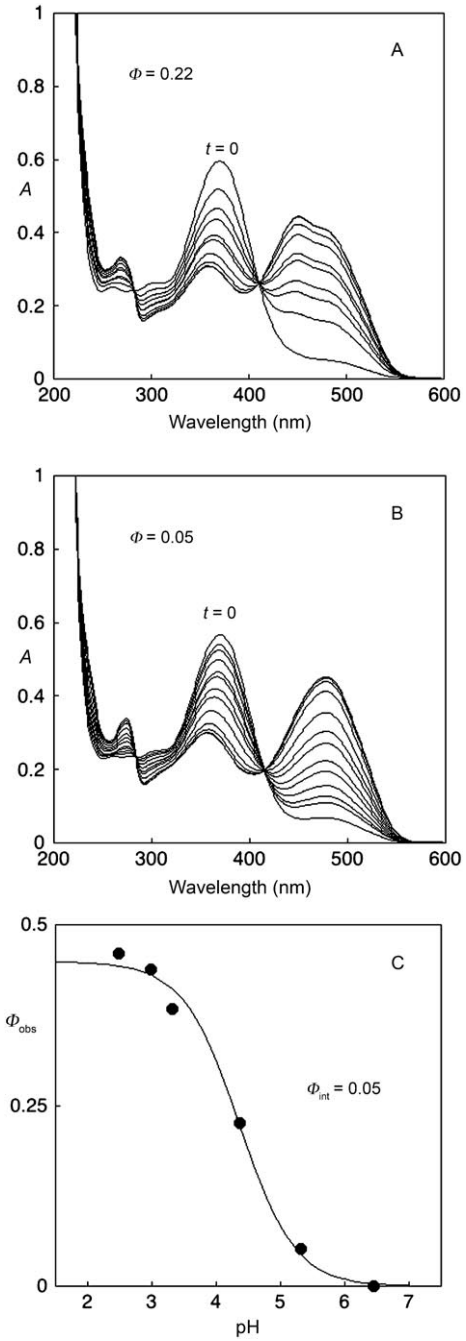

Figure 3. Spectral variations observed upon continuous irradiation (365 nm) of dark equilibrated solutions of **Ct** (4.17×10^{-5} M) as a function of time at pH 4.3 (A) and 5.3 (B). The quantum yields of formation of quinoidal base **A** and flavylium cation $\mathbf{AH^+}$ were calculated on the basis of the total light absorbed by the system and plotted as a function of the pH of the irradiated solution (C).

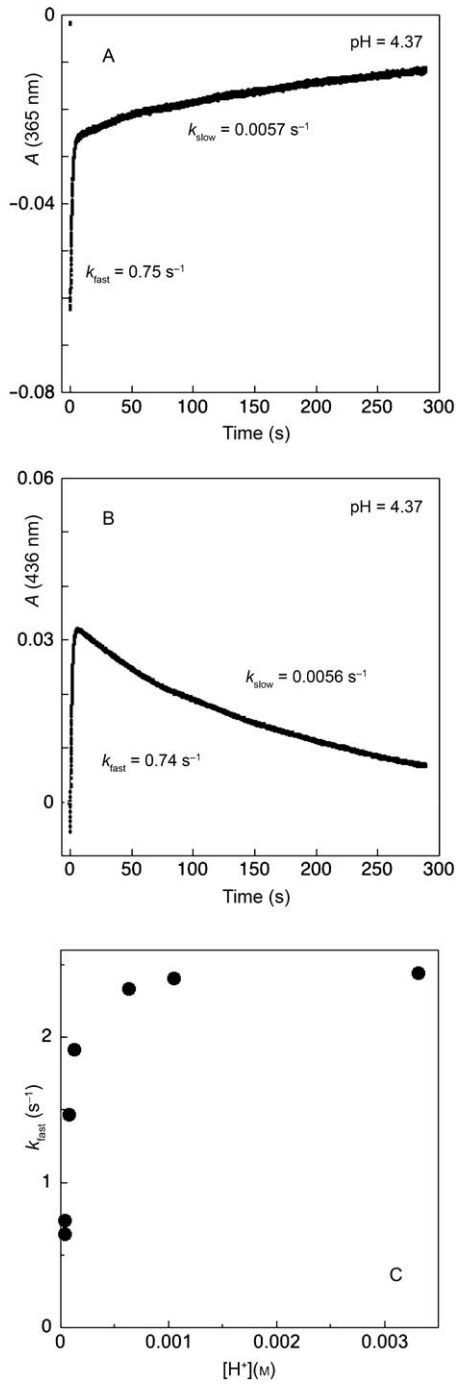

Figure 4. Time evolution of the absorbances at 365 nm (**Ct** absorption, A) and 436 nm (**AH+/A** absorption, B) upon flash irradiation of a solution of model compound **4** at pH 4.37. The rate constant for the fast process, k_{fast}, as a function of proton concentration is plotted in (C).

the hydration/dehydration and the proton dependence should be given by Equation (10).

$$k_{obs,fast\ (plateau)} = k_{-t} = 2.5\ s^{-1} \quad (9)$$

$$k_{obs,fast} = k_h + \frac{K_t k_i}{1+K_t} + \frac{k_{-h}[H^+]}{1+K_t} = 0.25 + 2.2\times 10^3[H^+] \quad (10)$$

The slower process reported in Figure 4A and B is the complete recovery of **Ct** and disappearance of $\mathbf{AH^+}$ to reach the initial equilibrium condition. It is the same kinetic process of the pH jumps and both follow Equation (7).

A global fitting of the data including time-resolved acid–base titrations in Figure 1 [Eqs. (11) and (12)], pH jump experiments yielding the bell-shaped curve in Figure 2B [Eq. (7)], quantum yields in Figure 3C [Eq. (8)], and flash photolysis experiments in Figure 4C [Eqs. (9) and (10)] allows us to calculate all the equilibrium and rate constants of the system, shown in Tables 1 and 2.

Table 1. Equilibrium constants for model compound **4** (water) and bis(flavylium) **3** (water/acetonitrile 80:20 v/v) at 295 K.

	K_h (M)	K_t	K_i	pK_a	pK'_a
model compound **4**	1.7×10^{-6}	4.8	200	4.1 (4.1)[a]	2.78 (2.85)[a]
bis(flavylium) **3**	1.4×10^{-5}	0.86	8.2×103	3.2 (3.2)[a]	1.0 (1.01)[a]

[a] Experimentally observed.

Table 2. Rate constants for model compound **4** (water) and bis(flavylium) **3** (water/acetonitrile 80:20 v/v) at 295 K.

	k_h [s^{-1}]	k_{-h} [M^{-1}s^{-1}]	k_t [s^{-1}]	k_{-t} [s^{-1}]	k_i [s^{-1}]	k_{-i} [s^{-1}]
model compound **4**	0.02	1.3×104	12	2.5	0.11	5×10^{-4}
bis(flavylium) **3**	0.26	1.9×104	1.25	1.45	1.0	1.2×10^{-4}

$$K_a = 10^{-4.1} \quad (11)$$

$$K'_a = K_a + K_h + K_h K_t + K_h K_t K_i = 10^{-2.85} \quad (12)$$

Bis(flavylium) 3

The network of chemical reactions: According to the model compound and following the behavior of other 7-hydroxyflavylium compounds[6] it is expected that each flavylium is involved in a fast equilibrium with its quinoidal base counterpart on one hand and that each hemiketal is in fast equilibrium with its *cis*-chalcone counterpart on the other. In other words, both hemiketal/*cis*-chalcone pairs are transient species not detected by ^{1}H NMR spectroscopy, as verified experimentally (see below). Each flavylium network can thus be viewed as an equilibrium involving $\mathbf{AH^+/A}$, a transient intermediate **X** (**B2** in fast equilibrium with **Cc**), and **Ct** ($\mathbf{AH^+/A}\rightleftarrows\mathbf{X}\rightleftarrows\mathbf{Ct}$; Scheme 3).

The question is if the two flavylium reaction networks have a stochastic behavior, that is, are they independent from each other or in spite of the methyleneviologen bridge separating them, the chemical changes taking place in one branch influence the other?

The study of the network of bis(flavylium) **3** was carried out by using an approach identical to the one used to study model compound **4**. Direct pH jumps from stock acidic solutions of the bis(flavylium) in a mixture of water and acetonitrile (80:20, v/v) to higher pH values were monitored immediately after the jump by UV/Vis spectrophotometry.

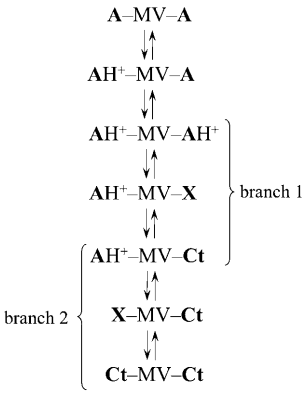

Scheme 3. Simplified network of chemical reactions arising from bis(flavylium) **3**.

The spectral characterization of the solutions immediately after the pH jumps was best carried out by stopped-flow since the high rate of the hydration reaction leads to the presence of already some **B** and **Cc** when the spectra are run in a common UV/Vis spectrophotometer instead of the dyode array spectrophotometer used in the stopped-flow equipment. Regarding the formation of the quinoidal base monitored at $\lambda_{max}(\mathbf{AH^+})=430$ and $\lambda_{max}(\mathbf{A})=480$ nm (Figure 5A), it was not possible to distinguish two separated pK_a values. This does not mean that they are equal since it is difficult to distinguish by spectrophotometry two pK_a values when they differ by less than one pH unit.[19] However, the experimental data of Figure 5A indicate that if the two pK_a values are not equal they are at least very close and thus the influence of the deprotonation in one branch of the compound has only a small effect on the other. Comparison of the pK_a of bis(flavylium) **3** (p$K_a=3.2$) with that of the model compound **4** (p$K_a=4.1$) reflects the effect of the positive charge of the viologen bridge on the 7-OH group making it more acidic. The same was observed for the global pK'_a. The global acidity constant defined by Equation (5) is higher for bis(flavylium) **3** (p$K'_a=1.0$) than for the model compound **4** (p$K'_a=2.85$). The fact that $\Delta pK'_a=1.85$ is larger than $\Delta pK_a=0.9$ probably reflects the closer proximity of the hydration point (C2) to the viologen when compared with the acidity point (OH in C7). The acidity constants of the chalcones in bis(flavylium) **3**, p$K_{Ct}=8.4$ and 10.0, compared with the values of 7.9 and 9.4, respectively, in the model compound **4**. This is only explained if the acidic form is relatively more stabilized than the basic one, and we do not have any reliable explanation unless to consider that the ionized chalcones are less stable in the solvent mixture used due to its zwitterionic character.

Solutions thermally equilibrated of bis(flavylium) **3** were made less acidic by addition of base and the respective kinetic processes followed by ^{1}H NMR spectroscopy. In Figure 6, a ^{1}H NMR spectrum run 32 min upon a pH jump to pH 1.6 is shown (see the Supporting Information for a complete set of data). This NMR spectroscopic data allows us to discriminate between the species $\mathbf{AH^+}$–MV–$\mathbf{AH^+}$ (all-flavylium), $\mathbf{AH^+}$–MV–**Ct**, and **Ct**–MV–**Ct** (all *trans*-chalcone). In particular, the methylene peaks of the MV spacer can be decomposed into the contributions from $\mathbf{AH^+}$–MV–$\mathbf{AH^+}$ (taken at low pH values or at the initial time of the pH jump), **Ct**–MV–**Ct** (at higher pH values after complete conversion of both $\mathbf{AH^+}$ moieties into **Ct**), and from the in-

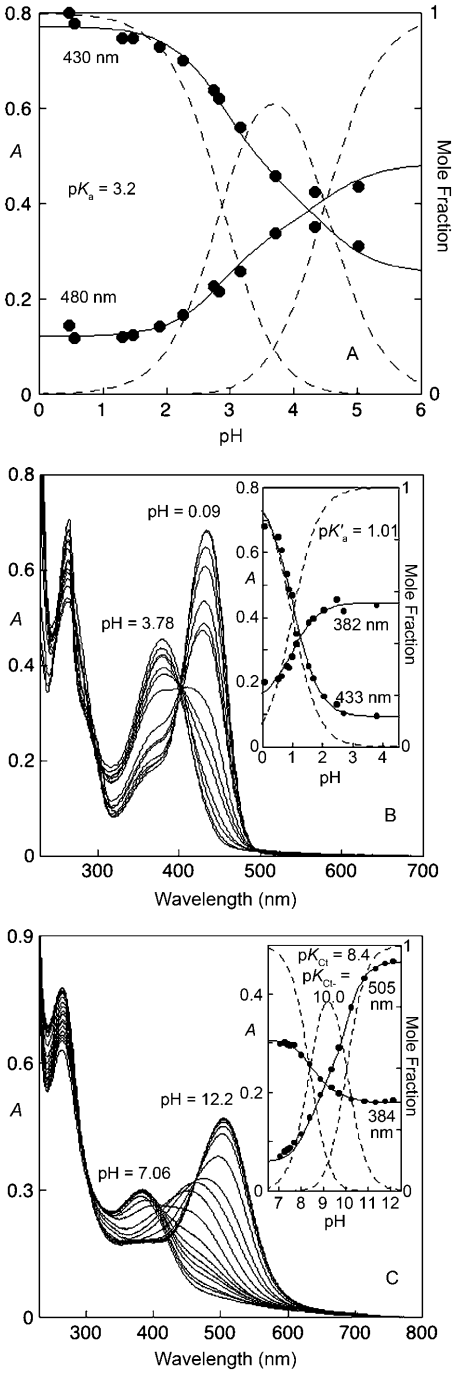

Figure 5. A) Absorbance data and/or absorption spectra of bis(flavylium) **3** immediately after a pH jump from a stock solution of 7.1×10^{-5} M at pH 0 to higher pH values; B) the same at the equilibrium. C) Spectral variations upon pH jumps of a solution at pH 12 ($\mathbf{Ct^{2-}}$) to less basic pH values, leading to the protonation of the *trans*-chalcones; fittings at 384 and 505 nm, with p*K*a values of 8.4 and 10.0. Solutions in water containing 20% acetonitrile.

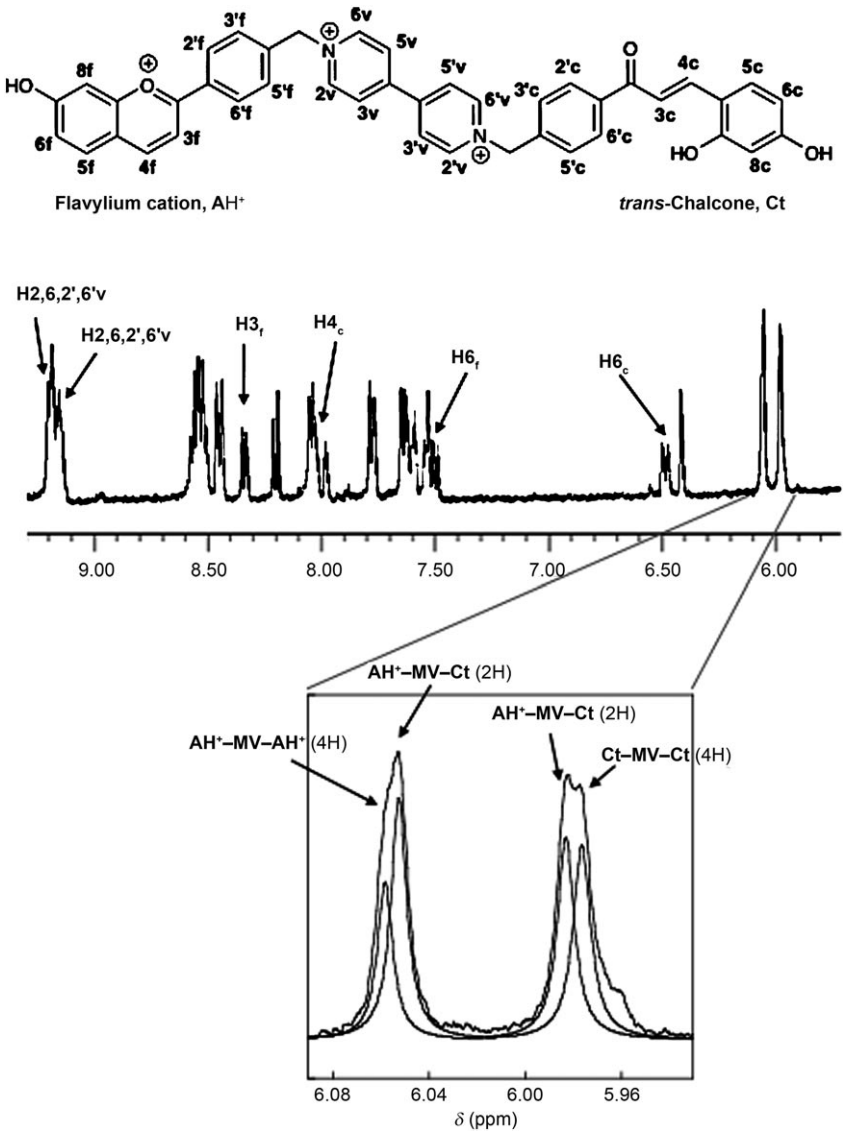

Figure 6. ^{1}H NMR spectrum of bis(flavylium) **3**, 32 min after of a pH jump from pH≈0 to 1.6. Decomposition of the signal of the methylene groups in Lorentzian curves is shown in the inset.

termediate **A**H$^+$–MV–**Ct** species. The decomposition was achieved by a global fitting of Lorentzian curves for different conversion times, as exemplified in Figure 6 (see also the Supporting Information) for $t=32$ min. The normalized areas of the Lorentzian curves allow calculation of the mole fraction of each species over time from which a kinetic analysis can be carried out.

In Figure 7A, the mole fraction distribution of the three species, **A**H$^+$–MV–**A**H$^+$, **A**H$^+$–MV–**Ct**, and **Ct**–MV–**Ct** were represented as a function of the fraction of the total **Cc**→**Ct** isomerization according to a stochastic behavior (——).[20] In the same figure, ----- indicate another limit situation in which all-flavylium **A**H$^+$–MV–**A**H$^+$ species was completely converted into **A**H$^+$–MV–**Ct** species before the isomerization of the other branch to give all-*trans*-chalcone **Ct**–MV–**Ct** species. The experimental data indicate that the present system deviates from the stochastic situation, which suggests some influence of the first isomerization into the second. This is also in accordance with the fact that the ^{1}H NMR spectra show small deviations that permitted us to characterize the three species. Another confirmation of this interpretation was obtained by fitting the mole fractions of the three components as a function of time, considering **A**H$^+$–MV–**A**H$^+$⇄**A**H$^+$–MV–**Ct**⇄**Ct**–MV–**Ct** (Figure 7B).[21,22] The rate constant of the first isomerization is approximately three times faster than the second one (6.3×10^{-4} vs. 2.3×10^{-4} s^{-1}, Figure 7B). In conclusion, the viologen bridge and the methylene spacers do not isolate both flavylium moieties from each other allowing their communication to some extent.

Finally, by using the data from Table 1 it is possible to construct an energy-level diagram (Figure 8) in which the relative position of the different species of the network are represented as previously reported from other flavylium networks.

Comparison between the two compounds indicates that in bis(flavylium) it is not only easier to remove the proton from the phenol, but also the hydration to give the hemiketal is more efficient. This can be explained by the effect of the positive charge of the bridge. On the other hand, the ring-opening implies a tautomerization reaction, that is, the transfer of a proton from the hydroxyl in the 2-position to the oxygen atom at the 1-position. This process is not favored by the positive charge of the bridge and by consequence **Cc** is less stable than **B2**. Finally the *cis*/*trans* isomerization is easier in the bis(flavylium), a result that is expected if the inductive effect of the bridge is considered.

Photochemistry: The photochemistry of the bis(*trans*-chalcone) of bis(flavylium) **3** is much less efficient than the one of the model compound **4** (Figure 9). Inspection of Table 1 gives some clues since the back reaction to restore *trans*-chalcone (k_i) is almost one order of magnitude faster in the former.

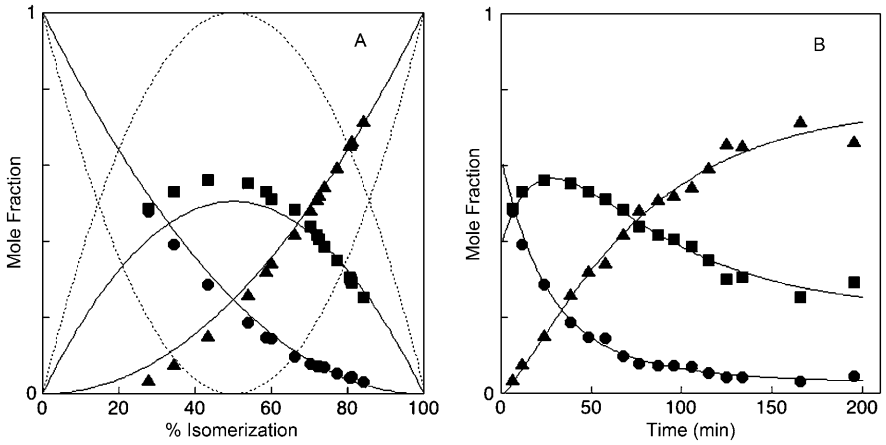

Figure 7. Mole fraction distribution of species $\mathbf{A}H^+$–MV–$\mathbf{A}H^+$ (●), **Ct**–MV–$\mathbf{A}H^+$ (■), and **Ct**–MV–**Ct** (▲) as a function of the total fraction of *trans*-chalcone moieties converted (A) and as a function of time (B). The fitting of the kinetic data was achieved by taking into account the reverse reaction in both isomerizations: 6.3×10^{-4} and $7.2\times10^{-5}\,s^{-1}$, respectively, for the direct and reverse reactions for the conversion of $\mathbf{A}H^+$–MV–$\mathbf{A}H^+$ into **Ct**–MV–$\mathbf{A}H^+$; 2.3×10^{-4} and $6.5\times10^{-5}\,s^{-1}$ for the analogous processes during the conversion of **Ct**–MV–$\mathbf{A}H^+$ into **Ct**–MV–**Ct**.

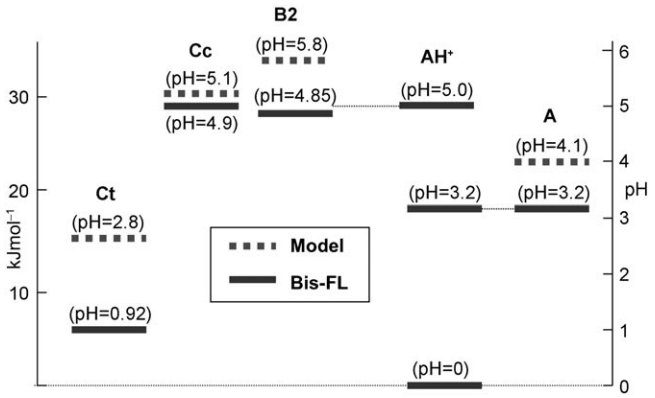

Figure 8. Combined energy-level diagram for bis(flavylium) **3** (water/acetonitrile 80:20 v/v) and model compound **4** (water); $T=295$ K.

Electrochemical studies: The flavylium cation is easily irreversibly reduced and by consequence the all *trans*-chalcone **Ct–Ct** species was used to carry out the electrochemical experiments. On the other hand, the methyl viologen (MV^{2+}) can be reversibly reduced to the blue radical cation ($MV^{+\bullet}$), which suggests the possibility of introducing a redox stimulus in the network. The formation of the methyl viologen radical was achieved by reducing a solution of **Ct–Ct** with dithionite, see Figure 10 (----- and blue–gray photo). The absorption spectrum is characteristic of the methyl viologen radical cation. The reversibility of the system was checked by addition of potassium peroxodisulphate, which recovers the absorption of the reduced form. However, the system is not completely reversible and some decomposition takes place, approximately 12% in one cycle.

Cyclic voltammetry was also performed. All cyclic voltammograms were run in aqueous solutions at pH 5.5 (acetate buffer 0.1 M; Figure 11, see the Supporting Information for individual voltammograms).

The *trans*-chalcone of the model compound shows two reduction peaks and an oxidation peak all corresponding to poorly reversible processes.[23,24] Regarding the **Ct**–MV–**Ct** species, the shape of the reduction peaks (see the Supporting Information) is identical to the one of the methyl viologen, although shifted to lower reduction potentials. Similarly, an analogous shift for the reduction peaks of the *trans*-chalcone moiety is expected. This means that the observed peaks for the **Ct**–MV–**Ct** species are superpositions of the reduction of the methyl viologen and the two **Ct** moieties. This also explains the lack of complete reversibility of the system.

Conclusions

The viologen unit has been shown to be a peculiar bridge linking two symmetric flavylium systems. The positive charge of the bridge has a significant effect on the properties of the flavylium moieties relative to the model compound 7-hydroxy-4'-methylflavylium: it favors the deprotonation and the hydration reactions, retards the tautomeriza-

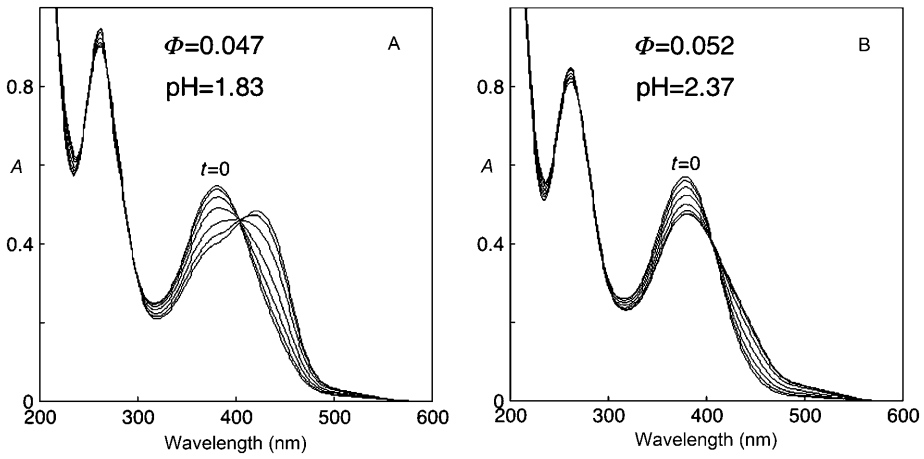

Figure 9. Spectral modifications upon irradiation at 365 nm of the bis(*trans*-chalcone) of bis(flavylium) **3**, $2.46\times10-5$ M in water/acetonitrile 80:20 v/v, at pH 1.83 (A) and 2.37 (B).

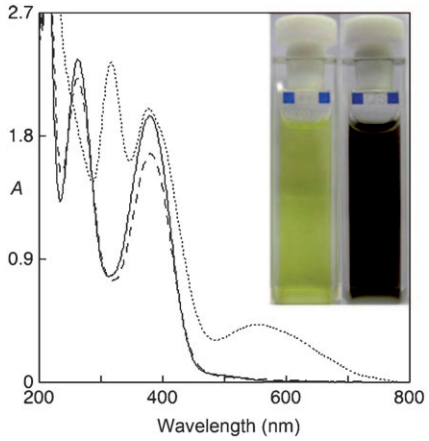

Figure 10. Reduction of bis(chalcone), **Ct**–MV–**Ct**, of **3** at pH 4.4 in 0.1 M acetate buffer (——, yellow color) with sodium dithionite (••••, blue–gray color); the system is partially reversible upon oxidation with potassium peroxodisulphate (-----).

tion, and enhances the isomerization. The methylene viologen bridge does not isolate both flavylium moieties from each other allowing their communication to some extent, as shown by the methylene ^{1}H NMR spectroscopic signals that allow us to distinguish between bis(flavylium), mixed flavylium-*trans*-chalcone, and all-*trans*-chalcone species. The bridge can also be electrochemically reduced permitting us to introduce a redox stimuli on the multistate network of the bis(flavylium) system, although it was not possible to carry out the reduction reversibly, a decomposition of 12% taking place in one cycle.

Experimental Section

Measurements: Solutions were prepared by using Millipore water and absolute ethanol (when needed). The pH of solutions was adjusted by addition of HCl, NaOH, or universal buffer of Theorell and Stenhagen[25] and pH was measured in a Radiometer Copenhagen PHM240 pH/ion meter. UV/Vis absorption spectra were recorded in a Varian-Cary 100 Bio spectrophotometer or in a Shimadzu VC2501-PC. Quantum yields were determined by irradiation at 365 nm, by using a medium pressure mercury arc lamp and the excitation bands were isolated with interference filters (Oriel). Actinometry was made by using the ferrioxalate system.[26]

General methods for synthesis: All reagents and solvents used were of analytical grade. NMR spectra were run on a Bruker AMX 400 instrument operating at 400.13 (^{1}H) and 100.00 MHz (^{13}C). COSY, HMQC, HMBC, and eventually NOESY spectra were run on each sample to allow full assignment of the NMR spectroscopic peaks. Mass spectra were run on an Applied Biosystems Voyager-DE PRO. Elemental analyses were obtained on a Thermofinnigan Flash EA 1112 Series instrument.

4′-Bromomethylacetophenone (1): 4′-Bromomethylacetophenone was prepared according to the method described by Leventis et al.[27] 4′-Methylacetophenone (14.9 mmol; 1.99 mL) was dissolved in CCl_4 (40 mL, carbon tetrachloride). NBS (16.37 mmol; 2.91 g) and AIBN (2.96 mmol; 0.486 g) were added. The resulting mixture was stirred and left in reflux for 4 days. The succinimide was filtered off, and the solvent removed under reduced pressure. The residue was purified by flash chromatography in hexane/ethyl ether (8:2) to yield 4′-bromomethylacetophenone (2.632 g, 12.35 mmol, 82.9%) as a yellow stable oil. ^{1}H NMR (CD_3OD, 400.13 MHz):[28] $\delta = 7.93$ (d, 2H, $^3J_{H2',H6'-H3',H5'} = 8.1$ Hz; $H_{2'}$, $H_{6'}$), 7.48 (d, 2H, $^3J_{H3',H5'-H2',H6'} = 7.9$ Hz; $H_{3'}$, $H_{5'}$), 4.50 (s, 2H; CH_2), 2.60 ppm (s, 3H; $COCH_3$); MS-MALDI/TOF+: *m*/*z*: calcd (%) for $C_9H_9BrO^+$: 211.98 (100); found: 211.1 $[M-H]^+$ (33.5), 212.1 $[M]^+$ (5).

1,1′-Di[(acetophenone-4-il)methyl]-4,4′-bipyridinium bromide (2): 1,1′-Di[(acetophenone-4-il)methyl]-4,4′-bipyridinium bromide was prepared according to the method described by Porter et al.[16] 4,4′-Bipiridil (2 mmol; 0.312 g) was dissolved in DMF (20 mL) in a round-bottomed flash containing a magnetic stir bar and a reflux condenser. The solution was degassed and placed under N_2. To the stirred solution, 4′-bromomethylacetophenone (6 mmol; 1.278 g) previously dissolved in DMF (6 mL) was added via syringe. The resulting mixture was stirred under N_2 and

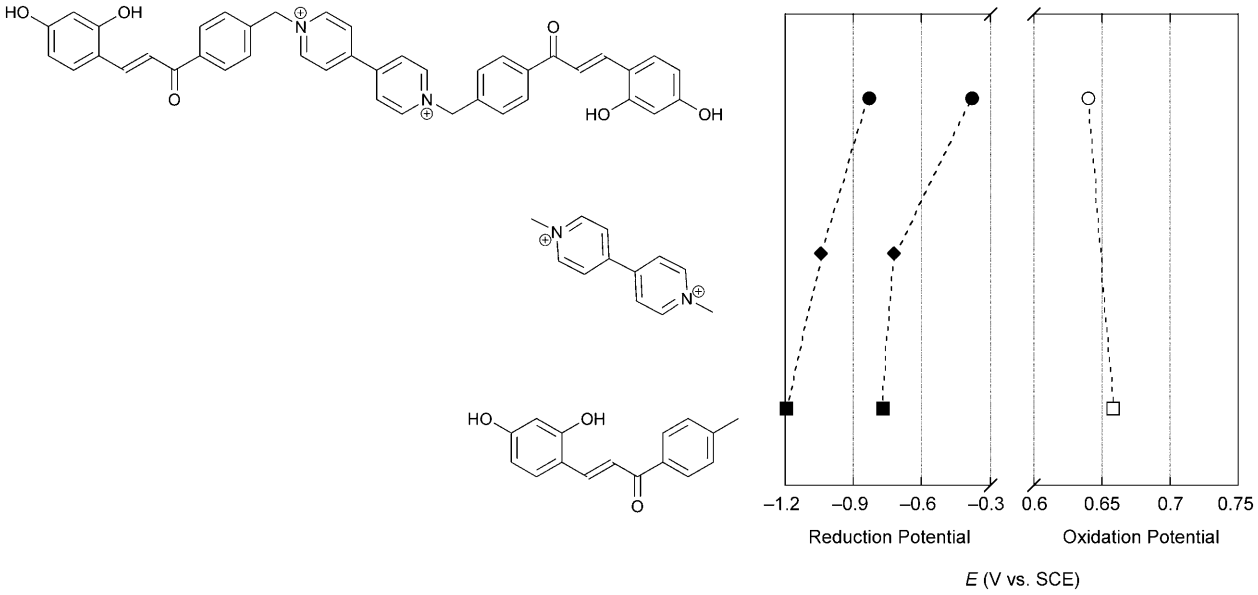

Figure 11. Reduction and oxidation potentials for the **Ct**–MV–**Ct** species of **3** and for model compounds MV and **4** (aqueous 0.1 M acetate buffer at pH 5.5) obtained from cyclic voltammetry carried out in a three-electrode cell with SCE as reference electrode, platinum wire as counter-electrode, and glassy carbon as the working electrode with a scan rate of 100 mV s^{-1}.

was allowed to reflux for 10 h and then concentrated by distillation. The crude was dissolved in methanol and an orange precipitate was obtained by adding ethyl ether. The solid was filtered off, washed with diethyl ether and dried, yielding 1,1′-di[(acetophenone-4-il)methyl]-4,4′-bipyridinium bromide (1.114 g, 1.91 mmol, 95.7%). ^{1}H NMR (CD_3OD, 400.13 MHz): δ = 9.36 (d, 4H, $^3J_{H2',H6',H2,H6-H3',H5',H3,H5}$ = 6.6 Hz; $H_{2'}$, $H_{6'}$, H_2, H_6), 8.70 (d, 4H, $^3J_{H3',H5',H2,H5-H2',H6',H2,H6}$ = 6.5 Hz; $H_{3'}$, $H_{5'}$, H_3, H_5), 8.09 (d, 4H, $^3J_{H9',H13',H9,H13-H10',H12',H10,H12}$ = 8.2 Hz; $H_{9'}$, $H_{13'}$, H_9, H_{13}), 7.67 (d, 4H, $^3J_{H10',H12',H10,H12-H9',H13',H9,H13}$ = 6.6 Hz; $H_{10'}$, $H_{12'}$, H_{10}, H_{12}), 6.05 (s, 4H; N-CH_2), 2.60 ppm (s, 6H; $COCH_3$); ^{13}C NMR (CD_3OD; 400.13 MHz): δ = 151.86 (C_4, $C_{4'}$), 147.37 (C_2, C_6, $C_{2'}$, $C_{6'}$), 139.56 (C_8, $C_{8'}$), 139.04 (C_{11}, $C_{11'}$), 130.58 (C_9, C_{13}, $C_{9'}$, $C_{13'}$), 130.45 (C_{10}, C_{12}, $C_{10'}$, $C_{12'}$), 128.73 (C_3, C_5, $C_{3'}$, $C_{5'}$), 65.26 (C_{N-CH2}), 26.79 ppm (C_{CH3}); MS-MALDI/TOF+: *m*/*z*: calcd (%) for $C_{28}H_{26}N_2O_2^+$: 422.20 (100); found: 289.5 $[M-C_9H_9O]^+$ (100); 421.6 $[M-H]^+$ (73); 423.5 $[M+H]^+$ (13); elemental analysis calcd (%) for $C_{28}H_{26}Br_2N_2O_2{\cdot}H_2O$: C 56.02, H 4.70, N 4.67; found: C 56.60, H 4.64, N 4.82.

1,1′-Di[(7-hydroxyflavylium-4′-il)methyl]-4,4′-bipyridinium perchlorate (3): 1,1′-Di[(acetophenone-4-il)methyl]-4,4′-bipyridinium bromide (0.2 mmol; 0.116 g) and 2,4-dihydroxybenzaldehyde (0.2 mmol; 0.027 g) were dissolved in glacial acetic acid (4 mL). Sulfuric acid (1.2 mL) was added and the resulting mixture was allow to stir overnight. A reddish solid was obtained by treating the solution with H_2O and perchloric acid. The solid was filtered off, washed with ethyl acetate, and dried, yielding 1,1′-di[(7-hydroxyflavylium-4′-il)methyl]-4,4′-bipyridinium perclorate (0.123 g, 0.12 mmol, 59.8%). ^{1}H NMR (DCl/CD_3OD, pD ≈ 1.0, 400.13 MHz): δ = 9.47 (d, 4H, $^3J_{H2',H6',H2,H6-H3',H5',H3,H5}$ = 6.6 Hz; $H_{2'}$, $H_{6'}$, H_2, H_6), 9.39 (d, 2H, $^3J_{H4f-H3f}$ = 8.3 Hz; H_{4f}), 8.78 (d, 4H, $^3J_{H3',H5',H3,H5-H2',H6',H2,H6}$ = 6.6 Hz; $H_{3'}$, $H_{5'}$, H_3, H_5), 8.59 (d, 4H, $^3J_{H3'f,H5'f-H2'f,H6'f}$ = 8.6 Hz; $H_{3'f}$, $H_{5'f}$), 8.58 (d, 2H, $^3J_{H3f-H4f}$ = 8.6 Hz; H_{3f}), 8.33 (d, 2H, $^3J_{H5f-H6f}$ = 9.0 Hz; H_{5f}), 7.96 (d, 4H, $^3J_{H2'f,H6f-H3'f,H5'f}$ = 8.2 Hz; $H_{2'f}$, $H_{6'f}$), 7.67 (s, 2H; H_{8f}), 7.55 (d, 2H, $^3J_{H6f-H5f}$ = 9.0, $^4J_{H6f-H8f}$ = 2.2 Hz; H_{6f}), 6.23 ppm (s, 4H; N−CH_2); MS-MALDI/TOF+: *m*/*z*: calcd (%) for $C_{42}H_{32}N_2O_4^+$: 628.24 (100); found: 627.7 $[M-H]^+$ (32.8); 391.7 $[M-C_{16}H_{13}O_2^+]^+$ (25); 235.6 $[M-C_{26}H_{20}N_2O_2^{3+}]^+$ (100); elemental analysis calcd (%) for $C_{42}H_{32}Cl_4N_2O_{20}{\cdot}3H_2O$: C 46.68, H 3.54, N 2.59; found: C 46.48, H 3.13, N 2.70.

7-Hydroxy-4′-methylflavylium tetrafluorborate (4): 7-Hydroxy-4′methylflavylium tetrafluorborate was prepared according to a procedure adapted from Katritzky. 2,4-Dihydroxybenzaldehyde (10 mmol, 1.38 g) and 4-methylacetophenone (10 mmol, 1.34 g) were dissolved in acetic acid (10 mL) and HBF_4 (2 mL). Acetic anhydride (10 mL) was then added dropwise and the temperature of the reaction raised. The reaction mixture was stirred overnight. By the following day diethyl ether and ethyl acetate were added and the orange solid precipitated was filtered off and carefully washed with diethyl ether and dried yielding 7-hydroxy-4′methylflavylium tetrafluorborate (0.57 g, 1.78 mmol, 18%). ^{1}H NMR (CD_3OD, 400.13 MHz): δ = 9.27 (d, 1H, $^3J_{H4,H3}$ = 8.5 Hz; H_4), 8.48 (d, 1H, $^3J_{H3,H4}$ = 8.5 Hz; H_4), 8.39 (d, 2H, $^3J_{H2',H6'-H3',H5'}$ = 8.3 Hz; $H_{2'6'}$), 8.25 (d, 1H, $^3J_{H5,H6}$ = 9.0 Hz; H_5), 7.62 (d, 1H, $^4J_{H8,H6}$ = 1.6 Hz; H_8), 7.56 (d, 2H, $^3J_{H3',H5'-H2',H6'}$ = 8.2 Hz; $H_{3'5}$), 7.49 ppm (d, 1H, $^3J_{H6,H5}$ = 9.0, $^3J_{H6,H8}$ = 2.0 Hz; H_6); ^{13}C NMR (CD_3OD; 400.13 MHz): δ = 173.55 (C_2), 171.36 (C_7), 161.15 (C_{8a}), 156.21 (C_4), 149.75 ($C_{4'}$), 134.44 (C_5), 132.05 ($C_{3'}$, $C_{5'}$), 130.61($C_{2'}$, $C_{6'}$), 127.81 (C_1), 123.46 (C_6), 121.29 (C_{4a}), 114.07 (C_3), 103.74 (C_8), 22.13 ppm (C_{CH3}).

Acknowledgements

We thank J. C. Lima and C. A. T. Laia for fruitful discussions and LabRMN at FCT-UNL and Rede Nacional de RMN (supported with funds from FCT-MCTES, Portugal) for access to the facilities. FCT-MCTES is also acknowledged for financial support through projects PTDC/QUI/67786/2006 and PTDC/QUI-QUI/104129/2008 and grants SFRH/BD/48226/2008 (A.D.) and SFRH/BPD/18214/2004 (V.P.).

[1] T. Swain in *The Flavonoids* (Eds.: J. B. Harborne, T. J. Mabry, H. Mabry), Chapman and Hall, London, **1975**, p. 1129.
[2] *Anthocyanins as Food Colors* (Ed.: P. Markakis), Academic Press, New York, **1982**.
[3] R. Brouillard, J.-E. Dubois, *J. Am. Chem. Soc.* **1977**, *99*, 1359–1364.
[4] R. McClelland, S. Gedge, *J. Am. Chem. Soc.* **1980**, *102*, 5838–5848.
[5] F. Pina, M. Maestri, V. Balzani in *Handbook of Photochemistry and Photobiology, Vol. 3*, American Scientific Publishers, Stevenson, **2003**, Chapter 9, pp. 411–449.
[6] F. Pina, M. J. Melo, A. J. Parola, M. Maestri, V. Balzani, *Chem. Eur. J.* **1998**, *4*, 2001–2007.
[7] M. J. Melo, F. Pina, C. Andary, *Anthocyanins, Nature's Glamorous Palette in Handbook of Natural Colorants* (Eds.: T. Bechtold, R. Mussak), Wiley, **2009**, pp. 135–150.
[8] M. J. Melo, A. J. Parola, J. C. Lima, F. Pina, *Chromogenic Materials Based on 2-Phenyl-1-benzopyrylium: From Anthocyanins to Synthetic Flavylium Compounds in Chromic Materials, Phenomena and their Technological Applications* (Ed.: P. R. Somani), RSC, London, **2010**, Chapter 16, pp. 537–576.
[9] F. Pina, J. C. Lima, A. J. Parola, C. A. M. Afonso, *Angew. Chem.* **2004**, *116*, 1551–1553; *Angew. Chem. Int. Ed.* **2004**, *43*, 1525–1527.
[10] L. Giestas, F. Folgosa, JC Lima, A. J. Parola, F. Pina, *Eur. J. Org. Chem.* **2005**, 4187–4200.
[11] M. C. Moncada, D. Fernandéz, J. C. Lima, A. J. Parola, C. Lodeiro, F. Folgosa, *Org. Biomol. Chem.* **2004**, *2*, 2802–2808.
[12] A. Roque, C. Lodeiro, F. Pina, M. Maestri, S. Dumas, P. Passaniti, *J. Am. Chem. Soc.* **2003**, *125*, 987–994.
[13] A. Roque, C. Lodeiro, F. Pina, M. Maestri, R. Ballardini, V. Balzani, *Eur. J. Org. Chem.* **2002**, 2699–2709.
[14] R. Robinson, D. D. Pratt, *J. Chem. Soc.* **1922**, 1577–1585.
[15] A. R. Katritzky, P. Czerney, J. R. Levell, W. Du, *Eur. J. Org. Chem.* **1998**, 2623–2629.
[16] W. W. Porter, T. P. Vaid, A. L. Rheingold, *J. Am. Chem. Soc.* **2005**, *127*, 16559.
[17] F. Galindo, J. C. Lima, S. V. Luis, A. J. Parola, F. Pina, *Adv. Funct. Mater.* **2005**, *15*, 541–545.
[18] R. Gomes, A. J. Parola, C. A. T. Laia, F. Pina, *Photochem. Photobiol. Sci.* **2007**, *6*, 1003–1009.
[19] J. T. Edsall, J. Wyman, *Biophysical Chemistry, Vol. 1*, Academic Press, New York, **1958**.
[20] A. Bencini, M. A. Bernardo, A. Bianchi, M. Ciampolini, V. Fusi, A. J. Parola, F. Pina, B. Valtancoli, *J. Chem. Soc. Perkin Trans. 2* **1998**, 413–418.
[21] K. A. Conners, *Chemical Kinetics The Study of Reaction Rates in Solution*, VCH, Weinheim, Chapter III, **1990**.
[22] V. Petrov, F. Pina, *J. Math. Chem.* **2010**, *47*, 1005–1026.
[23] L. D. Hicks, A. J. Fry, V. C. Kurzweil, *Electrochim. Acta* **2004**, *50*, 1039–1047.
[24] N. Cotelle, P. Hapiot, J. Pinson, C. Rolando, H. Vézin, *J. Phys. Chem. B* **2005**, *109*, 23720–23729.
[25] F. W. Küster, A. Thiel, *Tabelle per le Analisi Chimiche e Chimico-Fisiche*, 12nd ed., Hoepli, Milano, **1982**, pp. 157–160.
[26] C. G. Hatchard, C. A. Parker, *Proc. R. Soc. London Ser. A* **1956**, *235*, 518–536.
[27] N. Leventis, C. Sotiriou-Leventis, A. M. M. Rawashdeh, G. Zhang, *Electrochim. Acta* **2003**, *48*, 2799.
[28] See the Supporting Information for numeration of hydrogen and carbon atoms.

Received: December 24, 2010
Published online: April 19, 2011

